

# Efficient D-Xylose Hydrogenation to D-Xylitol over a Hydrotalcite-Supported Nickel Phosphide Nanoparticle Catalyst

Sho Yamaguchi,<sup>[a]</sup> Tomoo Mizugaki,<sup>[a, b]</sup> and Takato Mitsudome\*<sup>[a]</sup>

The hydrogenation of D-xylose is an industrially reliable method for preparing D-xylitol, which is a commonly consumed chemical. Herein, we report the highly efficient and selective hydrogenation of D-xylose to D-xylitol in water over a hydrotalcite (HT:  $\text{Mg}_6\text{Al}_2\text{CO}_3(\text{OH})_{16}\cdot 4(\text{H}_2\text{O})$ )-supported nickel phosphide nanoparticle catalyst (nano- $\text{Ni}_2\text{P}/\text{HT}$ ). The HT support drastically increased the catalytic activity of the nano- $\text{Ni}_2\text{P}$ , enabling D-xylitol synthesis under mild reaction conditions.

Notably, the selective hydrogenation of D-xylose to D-xylitol proceeded even under 1 bar of  $\text{H}_2$  or at room temperature for the first time. The nano- $\text{Ni}_2\text{P}/\text{HT}$  catalyst also exhibited the highest activity among previously reported non-noble metal catalysts, with a turnover number of 960. Moreover, the nano- $\text{Ni}_2\text{P}/\text{HT}$  catalyst was reusable and applicable to a concentrated D-xylose solution (50 wt%), demonstrating its high potential for the industrial production of D-xylitol.

## Introduction

D-Xylitol, which can be obtained from various biomass resources,<sup>[1]</sup> is valuable and ubiquitous in the food, cosmetic, and pharmaceutical industries.<sup>[2]</sup> For example, D-xylitol is the most popular “natural” sweetener in gums, sweets, and tooth-pastes, with an estimated 340 million dollar market, thereby representing one of the top-twelve value-added biomass derivatives.<sup>[3,4]</sup> The hydrogenation of D-xylose is a reliable method for the production of D-xylitol, because D-xylose can be obtained from the hydrolysis of beechwood hemicelluloses, which are one of the cheapest and most earth-abundant carbon resources. To date, this reaction has been performed over non-precious metal-based heterogeneous catalysts, such as Ni<sup>[5–9]</sup> and Co.<sup>[10]</sup> In this context, sponge Ni catalysts (Raney Ni catalysts) are widely used as industrial catalysts. However, sponge Ni catalysts suffer from low activities, requiring relatively high  $\text{H}_2$  pressures of 40–70 bar to give successful transformations.<sup>[11–14]</sup> Moreover, these catalysts have the serious drawback of pyrophoricity, rendering their handling difficult under an anaerobic atmosphere during the activation, operation, separation, and reuse of the catalysts.<sup>[15,16]</sup> Alternatively,

noble-metal-based catalysts, such as those based on Ru<sup>[17–26]</sup> and Pt,<sup>[27–29]</sup> have recently been studied for the hydrogenation of D-xylose, but the high costs and low abundances of these noble metals have severely impeded their application. Thus, the development of non-noble metal-based catalysts that are easy to handle and exhibit high activities, a lack of pyrophoricity, and can be readily reused is challenging. If such catalysts could be obtained, they would be expected to strongly contribute to the establishment of a green and sustainable D-xylose hydrogenation process.

In heterogeneous catalysts, such as supported metal nanoparticle catalysts, it is well known that the modulation of supports is crucial for designing highly active nanostructured catalysts, where the metal and support cooperatively function to activate the substrates and reagents in proximity.<sup>[30]</sup> However, cooperative catalysis between metal phosphides and supports has rarely been reported. Nevertheless, we recently developed supported non-precious metal phosphide nanoparticles for use in diverse hydrogenation reactions.<sup>[31–37]</sup> In particular, hydrotalcite (HT:  $\text{Mg}_6\text{Al}_2\text{CO}_3(\text{OH})_{16}\cdot 4(\text{H}_2\text{O})$ )-supported nickel phosphide nanoparticles (nano- $\text{Ni}_2\text{P}/\text{HT}$ ) served as a highly active, air-stable, and reusable catalyst for the hydrogenation of D-glucose and maltose to the corresponding sugar alcohols.<sup>[38,39]</sup> In this context, the combination of nano- $\text{Ni}_2\text{P}$  and HT played a key role in the high catalytic performance, where nano- $\text{Ni}_2\text{P}$  activates  $\text{H}_2$ , while HT acts as an electron donor to Ni and as an activator of the sugar C=O moiety, thereby facilitating the hydrogenation reaction. Focusing on the cooperative catalysis of nano- $\text{Ni}_2\text{P}/\text{HT}$ , we envisaged that the nano- $\text{Ni}_2\text{P}/\text{HT}$  catalyst would be applicable for the hydrogenation of D-xylose to D-xylitol. In this report, we demonstrate the use of nano- $\text{Ni}_2\text{P}/\text{HT}$  to catalyze the hydrogenation of D-xylose to obtain D-xylitol in water. The catalytic activity of nano- $\text{Ni}_2\text{P}/\text{HT}$  is evaluated under various conditions, including in a concentrated D-xylose solution (50 wt%), and is compared with those of

[a] Dr. S. Yamaguchi, Prof. Dr. T. Mizugaki, Dr. T. Mitsudome  
Department of Materials Engineering Science, Graduate School of Engineering Science  
Osaka University  
1-3 Machikaneyama, Toyonaka, Osaka 560-8531, Japan  
E-mail: mitsudom@cheng.es.osaka-u.ac.jp

[b] Prof. Dr. T. Mizugaki  
Innovative Catalysis Science Division, Institute for Open and Transdisciplinary Research Initiatives (ICS-OTRI)  
Osaka University  
Suita, Osaka 565-0871, Japan

Supporting information for this article is available on the WWW under <https://doi.org/10.1002/ejic.202100432>

Part of the [https://chemistry-europe.onlinelibrary.wiley.com/doi/toc/10.1002/\(ISSN\)1099-0682c.Supported-Catalysts](https://chemistry-europe.onlinelibrary.wiley.com/doi/toc/10.1002/(ISSN)1099-0682c.Supported-Catalysts) “Supported Catalysts” Special Collection.

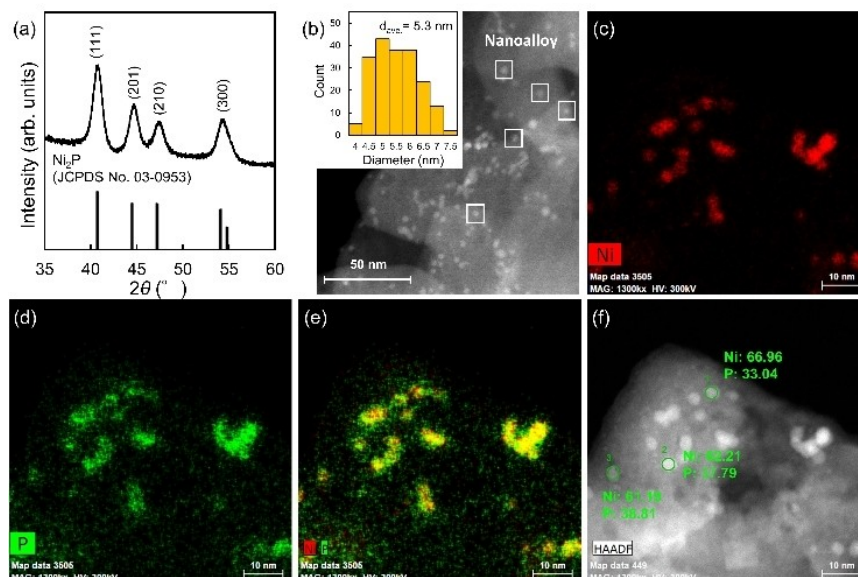


**Figure 1.** (a) XRD patterns of nano- $\text{Ni}_2\text{P}$  and  $\text{Ni}_2\text{P}$  (JCPDS No. 03-0953). (b) HAADF-STEM image of nano- $\text{Ni}_2\text{P}/\text{HT}$  (inset: size distribution histogram). Elemental mapping of (c) Ni and (d) P in nano- $\text{Ni}_2\text{P}/\text{HT}$ , and (e) composite overlay of (c) and (d). (f) EDX analysis of the nano- $\text{Ni}_2\text{P}$  particles on the HT support.

conventional Ni and Ru catalysts, in addition to other previously reported catalysts.

## Results and Discussion

The X-ray diffraction (XRD) pattern of nano- $\text{Ni}_2\text{P}$  displays four main peaks indexed to the hexagonal  $\text{Ni}_2\text{P}$  phase (JCPDS No. 03-0953) (Figure 1a).<sup>[40]</sup> A representative high-angle annular dark-field scanning transmission electron microscopy (HAADF-STEM) image of nano- $\text{Ni}_2\text{P}/\text{HT}$  shows the formation of spherical particles with an average diameter of 5.3 nm (Figure 1b). Energy-dispersive X-ray (EDX) spectroscopy with elemental mapping images confirmed the homogeneous distribution of Ni and P atoms in the nano- $\text{Ni}_2\text{P}$ , wherein the molar ratio of Ni to P was determined to be  $\sim 2:1$  (Figures 1c–1f). These results demonstrate that spherical  $\text{Ni}_2\text{P}$  nanoparticles are dispersed on the HT. In addition, the results of inductively coupled plasma atomic emission spectrometry (ICP-AES) revealed that the loading amount of Ni on the nano- $\text{Ni}_2\text{P}/\text{HT}$  is 0.91 wt% (Table S1). Furthermore, Figure 2 shows the X-ray photoelectron spectroscopy (XPS) results for the nano- $\text{Ni}_2\text{P}/\text{HT}$ . More specifically, Ni signals ascribed to  $\text{Ni } 2p_{3/2}$  and  $\text{Ni } 2p_{1/2}$  are detected at 852.4 and 869.4 eV, respectively, in the Ni 2p region (Figure 2a). These binding energies are similar to those of  $\text{Ni } 2p_{3/2}$  (852.6 eV) and  $\text{Ni } 2p_{1/2}$  (870.0 eV) for Ni metal.<sup>[41]</sup> On the other hand, the P 2p region displays two peaks at 129.2 and 132.3 eV (Figure 2b), wherein the binding energy of the former is close to that of  $\text{P}^0$  (130.0 eV), indicating that the state of P in nano- $\text{Ni}_2\text{P}/\text{HT}$  is  $\text{P}^{\delta-}$  ( $0 < \delta < 1$ ). The latter peak is ascribed to the  $\text{PO}_4^{3-}$  species arising from the superficial oxidation of nano- $\text{Ni}_2\text{P}$ . The Ni K-edge X-ray absorption near edge structure (XANES) spectrum of nano- $\text{Ni}_2\text{P}/\text{HT}$  is shown in Figure S1, along with those of Ni foil

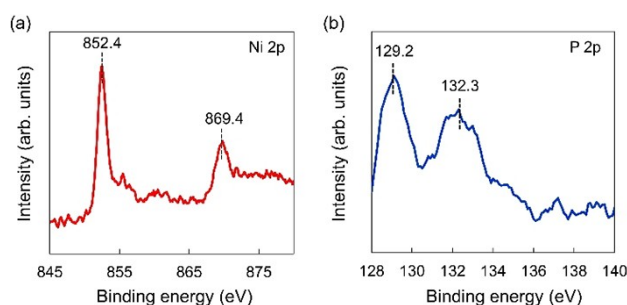
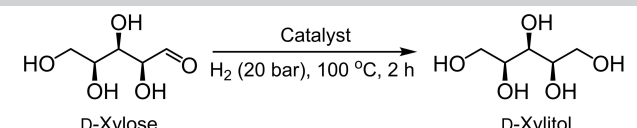


**Figure 2.** (a) Ni 2p and (b) P 2p XPS spectra of nano- $\text{Ni}_2\text{P}/\text{HT}$ .

and NiO as references.<sup>[38,39]</sup> The absorption edge energy of nano- $\text{Ni}_2\text{P}/\text{HT}$  was found to be close to that of Ni foil, thereby suggesting that the Ni species in nano- $\text{Ni}_2\text{P}/\text{HT}$  are present in a metal-like state, which is consistent with the XPS analysis.

The hydrogenation of D-xylose was then performed using supported and unsupported- $\text{Ni}_2\text{P}$  catalysts in water at 100 °C under 20 bar  $\text{H}_2$  (Table 1). It is noteworthy that nano- $\text{Ni}_2\text{P}/\text{HT}$  exhibited a high activity, affording D-xylitol in a  $>99\%$  yield (Table 1, entry 1). In sharp contrast, use of the unsupported nano- $\text{Ni}_2\text{P}$  resulted in almost no conversion of D-xylose (Table 1, entry 2). We also confirmed that HT itself did not produce D-xylitol but caused the isomerization of D-xylose to xylulose (Table 1, entry 3).<sup>[42]</sup> This demonstrates that the HT support drastically improved the catalytic activity of nano- $\text{Ni}_2\text{P}$  by more than 100 times. Importantly, nano- $\text{Ni}_2\text{P}/\text{HT}$  operated well under milder conditions than previously reported. Indeed, nano- $\text{Ni}_2\text{P}/\text{HT}$  is the first example of a catalyst for the efficient and high-yielding hydrogenation of D-xylose at ambient temperature or under 1 bar  $\text{H}_2$  pressure, when the appropriate catalyst amount,  $\text{H}_2$  pressure, and reaction time was employed for each condition

**Table 1.** Hydrogenation of D-xylose using various catalysts.<sup>[a]</sup>



Entry	Catalyst	D-Xylose conv. <sup>[b]</sup>	D-Xylitol yield <sup>[b]</sup>
1	nano-Ni <sub>2</sub> P/HT	> 99	> 99
2	nano-Ni <sub>2</sub> P	< 1	< 1
3	HT	37	< 1
4 <sup>[c]</sup>	nano-Ni <sub>2</sub> P/HT	> 99	> 99
5 <sup>[d]</sup>	nano-Ni <sub>2</sub> P/HT	99	87
6	nano-Ni <sub>2</sub> P/Al <sub>2</sub> O <sub>3</sub>	> 99	94
7	nano-Ni <sub>2</sub> P/MgO	> 99	47
8	nano-Ni <sub>2</sub> P/ZrO <sub>2</sub>	96	38
9	nano-Ni <sub>2</sub> P/TiO <sub>2</sub>	3	2
10	nano-Ni <sub>2</sub> P/SiO <sub>2</sub>	1	1
11	nano-Co <sub>2</sub> P/HT	49	4
12	Ni/HT	69	3
13	Ni/HT-Red	92	2
14	Raney Ni	39	39
15	Ru/C	99	94

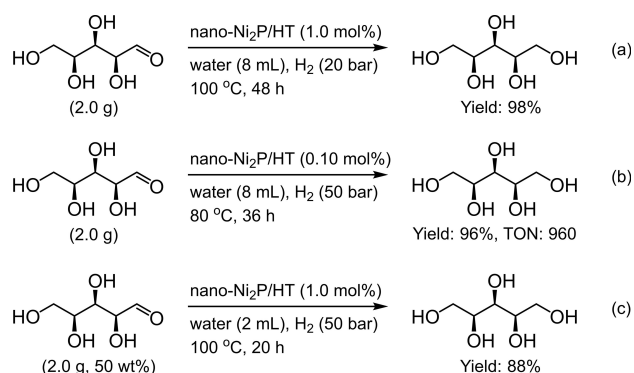
[a] Reaction conditions: D-xylose (0.5 mmol), catalyst (6.2 mol% metal), H<sub>2</sub>O (3 mL). [b] Determined by HPLC analysis using sucrose as the internal standard; given as %. [c] Catalyst (12.4 mol% Ni), H<sub>2</sub> (50 bar), 25 °C, 72 h. [d] H<sub>2</sub> (1 bar), 100 °C, 12 h.

(Table 1, entries 4 and 5). We also found that nano-Ni<sub>2</sub>P/Al<sub>2</sub>O<sub>3</sub> served as an active catalyst (Table 1, entry 6), while nano-Ni<sub>2</sub>P supported on MgO and ZrO<sub>2</sub> provided high conversions of D-xylose, although lower selectivities were obtained compared to the case of nano-Ni<sub>2</sub>P/HT (Table 1, entries 7 and 8) due to the formation of unidentified insoluble by-products (Table S2). TiO<sub>2</sub> and SiO<sub>2</sub> supports were not effective, resulting in low conversions of D-xylose (< 3%) (Table 1, entries 9 and 10). Unlike nano-Ni<sub>2</sub>P/HT, the nano-Co<sub>2</sub>P/HT catalyst provided only trace amounts of D-xylitol (Table 1, entry 11). These results clearly demonstrate that the combination of nano-Ni<sub>2</sub>P and the HT support is key to achieving the highly efficient and selective hydrogenation of D-xylose to D-xylitol. The high catalytic performance of nano-Ni<sub>2</sub>P/HT may be due to the cooperative catalysis by nano-Ni<sub>2</sub>P and HT, which activate H<sub>2</sub> and the C=O moiety of D-xylose, respectively.<sup>[35,38,39]</sup>

Subsequently, the catalytic activity of nano-Ni<sub>2</sub>P/HT in the hydrogenation of D-xylose was compared with those of conventional Ni catalysts. Ni/HT and its H<sub>2</sub>-treated Ni/HT-Red were investigated as model catalysts for NiO<sub>x</sub> and Ni(0) nanoparticles, respectively (Table 1, entries 12 and 13). Both catalysts resulted in extremely low yields of D-xylitol, accompanied by the production of an unidentified insoluble component. Raney Ni,<sup>[11–14]</sup> which is commonly used in industrial sugar hydrogenation processes, exhibited a high selectivity for D-xylitol, but its activity was significantly lower than that of nano-Ni<sub>2</sub>P/HT (Table 1, entry 14). Ru/C, which is a representative example of a commercially available noble metal catalyst, provided a slightly lower yield of D-xylitol than that obtained using nano-Ni<sub>2</sub>P/HT (Table 1, entry 15). These results suggest that the catalytic performance of nano-Ni<sub>2</sub>P/HT is comparable to those of noble metal-based catalysts.

A gram-scale hydrogenation of D-xylose with nano-Ni<sub>2</sub>P/HT (1.0 mol%) was then carried out, wherein 2.0 g of D-xylose was converted to D-xylitol in 98% yield (Scheme 1a). Interestingly, upon decreasing the amount of nano-Ni<sub>2</sub>P/HT to 0.10 mol%, 2.0 g of D-xylose was successfully converted to D-xylitol in 96% yield, with a turnover number (TON) of 960 (Scheme 1b). This TON value is the highest among those reported for non-noble metal catalysts.<sup>[5–8,10,12]</sup> Furthermore, the activity of nano-Ni<sub>2</sub>P/HT was tested in a concentrated D-xylose solution, since the applicability of such a catalyst to a concentrated solution is crucial for industrial applications. Notably, nano-Ni<sub>2</sub>P/HT operated well in a 50 wt% D-xylose solution to afford D-xylitol in 88% yield (Scheme 1c).

One of the most important advantages of heterogeneous catalysts is their convenient recyclability. However, previously reported non-noble metal catalysts for D-xylose hydrogenation have inevitably required pretreatment with H<sub>2</sub> at high temperatures for their activation. In contrast, nano-Ni<sub>2</sub>P/HT was easily recovered by filtration after the reaction and was found to be reusable without any necessity for pre-treatment. Indeed, four successive reaction cycles were achieved with a slight decrease in the D-xylitol yield (Figure 3a). To obtain more detailed information regarding the catalyst reusability, we further investigated the initial rate at an incomplete reaction time (30 min) in the recycling experiments. It was found that the yields of D-xylitol obtained at this point (diamond symbols in Figure 3a) using the fresh and reused catalysts were similar, indicating the durability of nano-Ni<sub>2</sub>P/HT. Furthermore, a hot-filtration experiment was performed to check the leaching of the metal species during the reaction (Figure 3b). After the removal of nano-Ni<sub>2</sub>P/HT by filtration at a 30% conversion of D-xylose, the filtrate was treated under similar reaction conditions, with no additional D-xylitol being observed in the filtrate. ICP-AES analyses showed that the amounts of Ni in the fresh and spent catalysts were the same, confirming that Ni leaching did not occur during D-xylose hydrogenation (Table S1). Following the reaction, XPS, TEM, and EDX were carried out to investigate the stability of the nano-Ni<sub>2</sub>P/HT catalyst. In the XPS Ni 2p spectrum of the spent nano-Ni<sub>2</sub>P/HT, two peaks can be seen at



**Scheme 1.** Gram-scale hydrogenation using (a) 1.0 mol% and (b) 0.10 mol% nano-Ni<sub>2</sub>P/HT. (c) Hydrogenation of D-xylose at a solution concentration of 50 wt%. The D-xylitol yield was determined by HPLC analysis using sucrose as the internal standard.

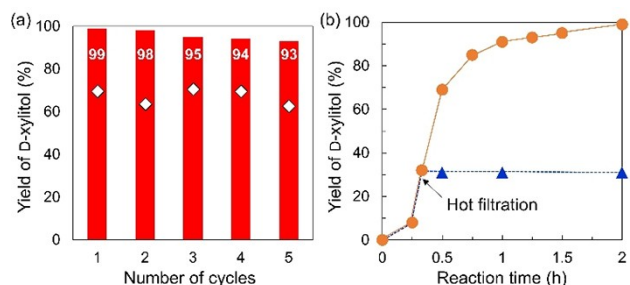


**Figure 3.** (a) Evaluation of the nano-Ni<sub>2</sub>P/HT-catalyzed hydrogenation of D-xylose over 5 catalytic cycles. Reaction conditions: D-xylose (0.25 mmol), nano-Ni<sub>2</sub>P/HT (200 mg, 6.2 mol% Ni) (0.91 wt% Ni loading), H<sub>2</sub>O (3 mL), H<sub>2</sub> (20 bar), 100 °C, reaction time = 2 h (red bars) or 30 min (white diamonds). (b) Hot filtration experiment of nano-Ni<sub>2</sub>P/HT: (orange dots) without filtration of the catalyst and (blue triangles) with removal of the catalyst by hot filtration after approximately 20 min. Reaction conditions: D-xylose (0.25 mmol), nano-Ni<sub>2</sub>P/HT (200 mg, 6.2 mol% Ni) (0.91 wt% Ni loading), H<sub>2</sub>O (3 mL), H<sub>2</sub> (20 bar), 100 °C.

852.4 and 869.4 eV, which are similar to those observed for the fresh nano-Ni<sub>2</sub>P/HT (Figure 2 and Figure S2). TEM and EDX analyses of the spent nano-Ni<sub>2</sub>P/HT show that both the average particle diameter and the Ni/P molar ratio of the spherical nano-Ni<sub>2</sub>P species are close to those of the fresh catalyst (Figure S3 and Figure S4). Overall, these results strongly support the high stability of the nano-Ni<sub>2</sub>P/HT catalyst.

Table 2 summarizes our comparison carried out between nano-Ni<sub>2</sub>P/HT and some previously reported non-noble metal catalysts in terms of their catalytic performances for the hydrogenation of D-xylose. nano-Ni<sub>2</sub>P/HT clearly outperformed the reported catalysts in terms of a quantitative synthesis of D-xylitol (Table 2, entry 1 vs. entries 6–12), mild operating conditions (Table 2, entries 2 and 3), applicability to a concentrated D-xylose solution (Table 2 entry 4 vs. entries 6 and 7), and a more than 10-fold higher TON value (Table 2, entry 5 vs. entry 6). Hence, nano-Ni<sub>2</sub>P/HT has great potential for use as an alternative to conventional catalysts for the production of D-xylitol.

## Conclusion

We achieved the highly efficient and selective hydrogenation of D-xylose to D-xylitol in water over an hydrotalcite (HT)-supported nickel phosphide (Ni<sub>2</sub>P) nanoparticle catalyst. Interestingly, while neither nano-Ni<sub>2</sub>P nor HT functioned as a catalyst, the nano-Ni<sub>2</sub>P/HT combination exhibited an excellent catalytic performance in the hydrogenation of D-xylose in terms of its activity and stability. The high activity of nano-Ni<sub>2</sub>P/HT was also demonstrated in the hydrogenation of D-xylose with only 1 bar of H<sub>2</sub> or at room temperature. Moreover, the success of the hydrogenation of a concentrated D-xylose solution (50 wt%), in addition to a high catalyst durability, and the easy handling of nano-Ni<sub>2</sub>P/HT verifies its potential for use in practical applications. Previously, cooperative catalysis between metal phosphides and supports has not been well studied; however, our results indicated that the combination of a metal phosphide and a support is a promising method for designing nanostructured catalysts with high activities and stabilities for diverse reaction applications.

## Experimental Section

### Preparation of nano-Ni<sub>2</sub>P/Support

Under an argon atmosphere, a Schlenk flask equipped with a stirring bar was charged with Ni(acac)<sub>2</sub> (1.0 mmol), CH<sub>3</sub>(CH<sub>2</sub>)<sub>15</sub>NH<sub>2</sub> (10 mmol), and P(OPh)<sub>3</sub> (10 mmol). The reaction mixture was heated to 315 °C at a rate of 30 °Cmin<sup>-1</sup> and maintained at this target temperature for 2 h. After cooling the reaction mixture to room temperature, acetone (10 mL) was added to precipitate the black solid which was then washed with a CHCl<sub>3</sub>-acetone (1:1, v/v) mixture (10 mL). The obtained solid was dried in vacuo to yield nano-Ni<sub>2</sub>P (90 mg) as a black powder. Loading nano-Ni<sub>2</sub>P on HT was as follows: HT (1.0 g) was added to a suspension of nano-Ni<sub>2</sub>P (30 mg) in *n*-hexane (100 mL). After stirring the mixture overnight at room temperature, the precipitate was filtered and the obtained solid was dried in vacuo to afford nano-Ni<sub>2</sub>P/HT (1.0 g) as a gray powder. For comparison of the catalytic activity of nano-Ni<sub>2</sub>P/HT with other catalysts, nano-Ni<sub>2</sub>P supported on other metal oxides (i.e., Al<sub>2</sub>O<sub>3</sub>, MgO, ZrO<sub>2</sub>, TiO<sub>2</sub>, or SiO<sub>2</sub>) in addition to Co phosphide nanoparticles supported on HT (nano-Co<sub>2</sub>P/HT), were also prepared in a similar manner to nano-Ni<sub>2</sub>P/HT (see the Supporting Information). Ni/HT and its H<sub>2</sub>-reduced form (Ni/HT-Red) were also

**Table 2.** Comparison with previous reports for the D-xylose hydrogenation reaction.

Entry	Catalyst	Conditions	D-xylitol yield [%]	TON	Ref.
1	nano-Ni <sub>2</sub> P/HT	2.4 wt% D-xylose, 6.2 mol% Ni, 100 °C, 20 bar H <sub>2</sub> , 2 h	> 99	16	<i>This work</i>
2	nano-Ni <sub>2</sub> P/HT	2.4 wt% D-xylose, 6.2 mol% Ni, 100 °C, 1 bar H <sub>2</sub> , 12 h	87	14	<i>This work</i>
3	nano-Ni <sub>2</sub> P/HT	2.4 wt% D-xylose, 12.4 mol% Ni, 25 °C, 50 bar H <sub>2</sub> , 72 h	> 99	8	<i>This work</i>
4	nano-Ni <sub>2</sub> P/HT	50 wt% D-xylose, 1.0 mol% Ni, 100 °C, 50 bar H <sub>2</sub> , 20 h	88	88	<i>This work</i>
5	nano-Ni <sub>2</sub> P/HT	20 wt% D-xylose, 0.1 mol% Ni, 80 °C, 50 bar H <sub>2</sub> , 36 h	96	960	<i>This work</i>
6	Co/SiO <sub>2</sub>	33 wt% D-xylose, 1.3 mol% Co, 140 °C, 50 bar H <sub>2</sub> , 4 h	90	71	[10]
7	Raney Ni	52 wt% D-xylose, 7.9 mol% Ni, 130 °C, 70 bar H <sub>2</sub> , 1–2 h	73	5	[12]
8	Nd <sub>0.5</sub> Ce <sub>0.5</sub> Al <sub>0.162</sub> Ni <sub>0.838</sub> O <sub>3</sub>	4.0 wt% D-xylose, 8.1 mol% Ni, 100 °C, 25 bar H <sub>2</sub> , 1–2 h	10	–	[7]
9	La <sub>0.3</sub> Ce <sub>0.7</sub> Al <sub>0.18</sub> Ni <sub>0.82</sub> O <sub>3</sub>	1.2 wt% D-xylose, 8.0 mol% Ni, 100 °C, 25 bar H <sub>2</sub> , 4 h	50	4	[5]
10	LaAl <sub>0.18</sub> Ni <sub>0.82</sub> O <sub>3</sub>	1.6 wt% D-xylose, 8.0 mol% Ni, 100 °C, 25 bar H <sub>2</sub> , 4 h	30	2	[6]
11	Raney Ni	4.8 wt% D-xylose, 9.3 mol% Ni, 100 °C, 40 bar H <sub>2</sub> , 2 h	62	6	[8]
12	Ni/SiO <sub>2</sub>	4.8 wt% D-xylose, 9.3 mol% Ni, 100 °C, 40 bar H <sub>2</sub> , 2 h	73	7	[8]



synthesized as models for the Ni(II) and Ni(0) catalysts, respectively (Figure S5 and Figure S6).

### Reaction Procedure

In a typical experiment (Table 1 entry 1), D-xylose (75 mg, 0.5 mmol), nano-Ni<sub>2</sub>P/HT (200 mg, 31 μmol Ni), and water (3 mL) were added to a 50 mL stainless steel autoclave equipped with a Teflon inner vessel. The reactor was closed, purged several times with H<sub>2</sub>, and pressurized at 20 bar. After heating at 100 °C for 2 h with stirring at 800 rpm, the autoclave was cooled to 25 °C, and H<sub>2</sub> gas was vented from the outlet. Sucrose was then added to the reaction mixture as an internal standard, the solid component was separated by centrifugation, and the reaction mixture was analyzed by HPLC. For further experimental details including experimental procedures and spectral data, see the Supporting Information.

### Acknowledgments

We thank Dr. Toshiaki Ina (SPRING-8) for carrying out the XAFS measurements (Grant Nos. 2020A0558 and 2020A1487) and Ryo Ota (Hokkaido University) for STEM analysis. This work was supported by JSPS KAKENHI Grant Nos. 18H01790, 20H02523, and 21K04776. This study was partially supported by the Cooperative Research Program of the Institute for Catalysis, Hokkaido University (Grant No. 21A1005). Part of this work was supported by the "Nanotechnology Platform" Program at Hokkaido University (Grant No. A-21-HK-0051) and the Nanotechnology Open Facilities in Osaka University (Grant No. A-20-OS-0025) of the Ministry of Education, Culture, Sports, Science and Technology (MEXT), Japan.

### Conflict of Interest

The authors declare no conflict of interest.

**Keywords:** Heterogeneous catalysis · Hydrogenation · Nickel phosphide · D-Xylose · D-Xylitol

- [1] J. Holladay, J. Bozell, J. White, D. Johnson, Top value-added chemicals from biomass. DOE Report PNNL 16983 **2007**.
- [2] Y. D. Arcaño, O. D. V. García, D. Mandelli, W. A. Carvalho, L. A. M. Pontes, *Catal. Today* **2020**, *344*, 2–14.
- [3] A. Sokmen, G. Gunes, *LWT-Food Sci. Technol.* **2006**, *39*, 1053–1058.
- [4] A. P. Tathod, P. L. Dhepe, *Green Chem.* **2014**, *16*, 4944–4954.
- [5] R. Morales, C. H. Campos, J. L. G. Fierro, M. A. Fraga, G. Pecchi, *RSC Adv.* **2016**, *6*, 67817–67826.
- [6] R. Morales, C. H. Campos, J. L. G. Fierro, M. A. Fraga, G. Pecchi, *J. Mol. Catal.* **2017**, *436*, 182–189.
- [7] R. Morales, C. H. Campos, J. L. G. Fierro, M. A. Fraga, G. Pecchi, *Catal. Today* **2018**, *310*, 59–67.
- [8] Hong Du, X. Ma, M. Jiang, P. Yan, Y. Zhao, Z. C. Zhang, *Catal. Today* **2021**, *365*, 265–273.
- [9] H. Xia, L. Zhang, H. Hu, S. Zuo, L. Yang, *Nanomaterials* **2020**, *10*, 73.
- [10] M. Audemar, W. Ramdani, T. Junhui, A. R. Ifrim, A. Ungureanu, F. Jérôme, S. Royer, K. Oliveira Vigier, *ChemCatChem* **2020**, *12*, 1973–1978.
- [11] J.-P. Mikkola, T. Salmi, R. Sjöholm, *J. Chem. Technol. Biotechnol.* **1999**, *74*, 655–662.
- [12] J.-P. Mikkola, H. Vainio, T. Salmi, R. Sjöholm, T. Ollonqvist, J. Väyrynen, *Appl. Catal. A* **2000**, *196*, 143–155.
- [13] J.-P. Mikkola, T. Salmi, R. Sjöholm, *J. Chem. Technol. Biotechnol.* **2001**, *76*, 90–100.
- [14] A. Fehér, C. Fehér, M. Rozbach, G. Rácz, M. Fekete, L. Hegedűs, Z. Barta, *Chem. Eng. Technol.* **2018**, *41*, 496–503.
- [15] V. Boschhat, P. Leconte, **1999**, FR2773086.
- [16] M. Endo, Y. Kuroda, **2001**, JP2001079411.
- [17] D. K. Mishra, A. A. Dabbawala, J.-S. Hwang, *Appl. Catal. A* **2012**, *425–426*, 110–116.
- [18] V. V. Ordmsky, J. C. Schouten, J. van der Schaaf, T. A. Nijhuis, *Appl. Catal. A* **2013**, *451*, 6–13.
- [19] D. K. Mishra, A. A. Dabbawala, J.-S. Hwang, *Catal. Commun.* **2013**, *41*, 52–55.
- [20] J. Lee, Y. T. Kim, G. W. Huber, *Green Chem.* **2014**, *16*, 708–718.
- [21] D. K. Mishra, A. A. Dabbawala, J.-S. Hwang, *J. Mol. Catal. A* **2013**, *376*, 63–70.
- [22] T. N. Pham, A. Samikannu, A.-R. Rautio, K. L. Juhasz, Z. Konya, J. Wärnå, K. Kordas, J.-P. Mikkola, *Top. Catal.* **2016**, *59*, 1165–1177.
- [23] C. Hernandez-Mejia, E. S. Gnanakumar, A. Olivos-Suarez, J. Gascon, H. F. Greer, W. Zhou, G. Rothenberg, N. Raveendran Shiju, *Catal. Sci. Technol.* **2016**, *6*, 577–582.
- [24] N. Sánchez-Bastardo, I. Delidovich, E. Alonso, *ACS Sustainable Chem. Eng.* **2018**, *6*, 11930–11938.
- [25] X.-J. Zhang, H.-W. Li, W. Bin, B.-J. Dou, D.-S. Chen, X.-P. Cheng, M. Li, H.-Y. Wang, K.-Q. Chen, L.-Q. Jin, Z.-Q. Liu, Y.-G. Zheng, *J. Agric. Food Chem.* **2020**, *68*, 12393–12399.
- [26] J. J. Musci, M. Montaña, E. Rodríguez-Castellón, I. D. Lick, M. L. Casella, *J. Mol. Catal.* **2020**, *495*, 111150.
- [27] A. Tathod, T. Kane, E. S. Sanil, P. L. Dhepe, *J. Mol. Catal. A* **2014**, *388–389*, 90–99.
- [28] N. P. Tangale, P. S. Niphadkar, P. N. Joshi, P. L. Dhepe, *Catal. Sci. Technol.* **2018**, *8*, 6429–6440.
- [29] N. P. Tangale, P. S. Niphadkar, P. N. Joshi, P. L. Dhepe, *Microporous Mesoporous Mater.* **2019**, *278*, 70–80.
- [30] K. Kaneda, T. Mitsudome, *Chem. Rec.* **2017**, *17*, 4–26.
- [31] S. Fujita, K. Nakajima, J. Yamasaki, T. Mizugaki, K. Jitsukawa, T. Mitsudome, *ACS Catal.* **2020**, *10*, 4261–4267.
- [32] T. Mitsudome, M. Sheng, A. Nakata, J. Yamasaki, T. Mizugaki, K. Jitsukawa, *Chem. Sci.* **2020**, *11*, 6682–6689.
- [33] S. Fujita, S. Yamaguchi, S. Yamazoe, J. Yamasaki, T. Mizugaki, T. Mitsudome, *Org. Biomol. Chem.* **2020**, *18*, 8827–8833.
- [34] H. Ishikawa, M. Sheng, A. Nakata, K. Nakajima, S. Yamazoe, J. Yamasaki, S. Yamaguchi, T. Mizugaki, T. Mitsudome, *ACS Catal.* **2021**, *11*, 750–757.
- [35] S. Fujita, S. Yamaguchi, J. Yamasaki, K. Nakajima, S. Yamazoe, T. Mizugaki, T. Mitsudome, *Chem. Eur. J.* **2021**, *27*, 4439–4446.
- [36] M. Sheng, S. Fujita, S. Yamaguchi, J. Yamasaki, K. Nakajima, S. Yamazoe, T. Mizugaki, T. Mitsudome, *JACS Au* **2021**, *1*, 501–507.
- [37] S. Fujita, K. Imagawa, S. Yamaguchi, J. Yamasaki, S. Yamazoe, T. Mizugaki, T. Mitsudome, *Sci. Rep.* **2021**, *11*, 10673.
- [38] S. Yamaguchi, S. Fujita, K. Nakajima, S. Yamazoe, J. Yamasaki, T. Mizugaki, T. Mitsudome, *Green Chem.* **2021**, *23*, 2010–2016.
- [39] S. Yamaguchi, S. Fujita, K. Nakajima, S. Yamazoe, J. Yamasaki, T. Mizugaki, T. Mitsudome, *ACS Sustainable Chem. Eng.* **2021**, *9*, 6347–6354.
- [40] Y. Pan, Y. Liu, J. Zhao, K. Yang, J. Liang, D. Liu, W. Hu, D. Liu, Y. Liu, C. Liu, *J. Mater. Chem. A* **2015**, *3*, 1656–1665.
- [41] B. V. Crist, *Handbooks of Monochromatic XPS Spectra. Volume 1 - The Elements and Native Oxides*. XPS International, LLC **1999**.
- [42] M. Paniagua, S. Saravanamurugan, M. Melian-Rodríguez, J. A. Melero, A. Riisager, *ChemSusChem* **2015**, *8*, 1088–1094.

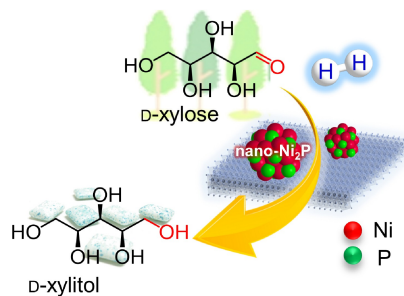
Manuscript received: May 18, 2021

Revised manuscript received: June 24, 2021

Accepted manuscript online: June 29, 2021

## FULL PAPERS

The hydrogenation of D-xylose to D-xylitol proceeded efficiently over hydrotalcite-supported nickel phosphide nanoparticles (nano-Ni<sub>2</sub>P/HT), which outperformed conventional catalysts and enabled D-xylose hydrogenation even under 1 bar H<sub>2</sub> or ambient temperature for the first time. Moreover, nano-Ni<sub>2</sub>P/HT was reusable, and operated well in a concentrated D-xylose solution (50 wt %).



- ☑ High activity, stability, and reusability
- ☑ Applicability for a concentrated solution

Dr. S. Yamaguchi, Prof. Dr. T. Mizugaki,  
Dr. T. Mitsudome\*

1 – 6

**Efficient D-Xylose Hydrogenation to D-Xylitol over a Hydrotalcite-Supported Nickel Phosphide Nanoparticle Catalyst**

